

The Convex Matching Distance in Multiparameter Persistence

Patrizio Frosini Ulderico Fugacci Eloy Mosig García Nicola Quercioli
 Sara Scaramuccia Francesca Tombari

Abstract

We introduce the convex matching distance, a novel metric for comparing functions with values in the real plane. This metric measures the maximal bottleneck distance between the persistence diagrams associated with the convex combinations of the two function components. Similarly to the traditional matching distance, the convex matching distance aggregates the information provided by two real-valued components. However, whereas the matching distance depends on two parameters, the convex matching distance depends on only one, offering improved computational efficiency. We further show that the convex matching distance can be more discriminative than the traditional matching distance in certain cases, although the two metrics are generally not comparable. Moreover, we prove that the convex matching distance is stable and characterize the coefficients of the convex combination at which it is attained. Finally, we demonstrate that this new aggregation framework benefits from the computational advantages provided by the Pareto grid, a collection of curves in the plane whose points lie in the image of the Pareto critical set associated with functions assuming values on the real plane.

Keywords

Biparameter persistent homology, Matching distance, Pareto grid.

1 Introduction

In recent years, research on multiparameter persistent homology has grown substantially, driven by the need to apply Topological Data Analysis (TDA) techniques to data represented by multifiltrations, as occurs, for example, when analysing or comparing data described by vector-valued functions [27, 4, 13, 10, 12, 11, 14, 19, 15, 18, 31, 1, 28]. However, a fully developed theoretical framework enabling efficient applications of TDA in this setting is still lacking. A widely adopted comparison method in multiparameter persistence is based on the *matching distance* [22, 5, 16, 29, 2, 6]. This pseudo-metric is introduced by observing that, given a continuous function $\varphi : X \rightarrow \mathbb{R}^n$ representing the data of interest, we can consider monoparametric filtrations of the topological space X associated with lines in \mathbb{R}^n having direction given by a vector $\mathbf{a} = (a_1, \dots, a_n)$ such that $\sum_{i=1}^n a_i = 1$ and $a_1, \dots, a_n \geq 0$. Each such line, parametrised as $\mathbf{b} + u\mathbf{a}$ with $\mathbf{b} = (b_1, \dots, b_n)$ and $\sum_{i=1}^n b_i = 0$, induces a filtration $\{X_u^{(\mathbf{a}, \mathbf{b})}\}_{u \in \mathbb{R}}$ of X defined by the subsets $X_u^{(\mathbf{a}, \mathbf{b})}$ consisting of all points in X whose image under φ has coordinates less than or equal to those of $\mathbf{b} + u\mathbf{a}$. From an analytical viewpoint, this construction is equivalent to considering, for each function $\varphi = (\varphi_1, \dots, \varphi_n) : X \rightarrow \mathbb{R}^n$, the sublevel sets of the real-valued function

$$\varphi_{\mathbf{a}, \mathbf{b}}^*(p) := \min_{1 \leq i \leq n} \{a_i\} \max_{1 \leq i \leq n} \left\{ \frac{\varphi_i(p) - b_i}{a_i} \right\}. \quad (1)$$

With this premise, the matching distance in degree k between two continuous functions $\varphi, \psi : X \rightarrow \mathbb{R}^n$ is defined by setting

$$d_{\text{match}, k}(\varphi, \psi) := \sup_{\mathbf{a}, \mathbf{b}} d_B \left(\text{Dgm}_k \left(\varphi_{\mathbf{a}, \mathbf{b}}^* \right), \text{Dgm}_k \left(\psi_{\mathbf{a}, \mathbf{b}}^* \right) \right),$$

where d_B is the bottleneck distance and Dgm_k is the operator that computes the persistence diagrams in degree k .

In recent years, the extended Pareto Grid has been introduced to compute points in the persistence diagram of $\varphi_{\mathbf{a}, \mathbf{b}}^*$, and to characterise at which (\mathbf{a}, \mathbf{b}) the matching distance is attained [17, 23, 26].

While the study of the matching distance is geometrically interesting and theoretically rich it involves $2(n-1)$ independent parameters and depends non-smoothly on the function φ , leading to computational challenges and monodromy [17]. We address this issue by considering the operator that maps a function

$$\varphi = (\varphi_1, \dots, \varphi_n) : X \rightarrow \mathbb{R}^n$$

to a family of real-valued functions φ^t defined as follows: for each $\mathbf{t} = (t_1, \dots, t_n) \in \mathbb{R}^n$ satisfying $\sum_{i=1}^n t_i = 1$ and $t_i \geq 0$ for all i , we set

$$\varphi^t := \sum_{i=1}^n t_i \varphi_i.$$

The conditions on \mathbf{t} imply $t_n = 1 - \sum_{i=1}^{n-1} t_i$; hence, the family $\{\varphi^t\}_{t \in \mathbb{R}^n}$ depends on $n-1$ parameters, substantially reducing the complexity of the approach based on the parameters \mathbf{a} and \mathbf{b} . Moreover, our operator $F_t(\varphi) = \varphi^t$ depends smoothly on the parameters \mathbf{t} and the function φ , in contrast with the operator in (1).

Furthermore, the operator F_t gives rise to a new pseudo-metric between filtering functions, called the *convex matching distance*, defined as

$$\text{cmd}_k(\varphi, \psi) := \max_{\substack{t_1, \dots, t_n \geq 0 \\ t_1 + \dots + t_n = 1}} d_B(\text{Dgm}_k(\varphi^t), \text{Dgm}_k(\psi^t)).$$

Although this pseudo-metric is not always more discriminative than the classical matching distance (as shown by Examples 1 and 2), its dependence on $n-1$ parameters, together with the fact that it is defined via a smooth procedure, provides significant computational advantages from an applied perspective.

In this paper, we focus on the case $n = 2$. We prove that the convex matching distance is stable with respect to the uniform norm $\|\varphi - \psi\|_\infty$ (Proposition 2) and establish a *Position Theorem* (Theorem 2), analogous to the one already known for the matching distance [17, 26]. This theorem allows one to recover, from the Pareto grid of φ , the coordinates of the points in the persistence diagram of $\varphi^t := (1-t)\varphi_1 + t\varphi_2$, for every $t \in [0, 1]$. Finally, in Theorem 3, we show that the convex matching distance coincides with the maximal bottleneck distance between the persistence diagrams of the functions φ^t and ψ^t for t belonging to a suitable set of special values, thus paving the way for an efficient method to compute the convex matching distance.

The proposed strategy can be reinterpreted within the framework of *Group Equivariant Non-Expansive Operators* (GENEOs). Our new pseudo-metric is indeed associated with the GENEO F_t that maps each function φ to the function φ^t . GENEOs have been employed in TDA to tune the invariance properties of persistence diagrams to the requirements of specific applications [25], and in geometric and topological deep learning to design efficient neural architectures [3, 7, 8, 9, 30, 21].

Interestingly, infinitely many other examples of parametric families of GENEOs can be defined. For instance:

$$\hat{F}_t(\varphi) := (1-t) \max(\varphi_1, \varphi_2) + t \min(\varphi_1, \varphi_2), \quad t \in [0, 1],$$

and

$$\tilde{F}_t(\varphi) := \left(\frac{1}{2} |\varphi_1|^t + \frac{1}{2} |\varphi_2|^t \right)^{\frac{1}{t}}, \quad t \geq 1.$$

Each of these operators could be used to define new pseudo-metrics in TDA.

The approach described in this paper is related to, but distinct from, the *persistent homology transform* (PHT) [33]. The PHT is a topological transform that takes as input a subset of a Euclidean space and associates to every unit vector the collection of persistence diagrams of the height functions on that subset in the direction given by the vector. A distance between two subsets is then defined by integrating over the sphere the distances between the respective persistence diagrams. The convex matching distance, instead, is obtained as a maximum over the unit vectors of non-negative slope, thus, over a smaller set. Considering only vectors of positive slope is a crucial aspect of our techniques because, together with some regularity assumptions, it enables the use of a convenient differential geometry tool, called the *Pareto grid*. Another key difference between the two approaches lies in their scope. While the PHT is designed to recover the geometry of the object X , our method, based on convex combinations of a vector-valued function, focuses on making inferences about the function whose domain is X .

2 Preliminaries

In this section, we recall the bottleneck distance in monoparameter persistence and the matching distance in biparameter persistence. To do that, some preliminary notions about persistence theory is needed,

and certain hypothesis need to be assumed. However, as this is fairly standard, we will not delve into details, and refer the reader to [26, Section 2 and Appendix A] for a compact treatment of preliminaries. The following is a complete list of symbols used in this article ¹:

- X is a compact topological space;
- $\Delta := \{(u, u) \mid u \in \mathbb{R}\}$, $\Delta^+ := \{(u, v) \mid u, v \in \mathbb{R}, u < v\}$, $\bar{\Delta}^* := \Delta^+ \cup \{(u, \infty) \mid u \in \mathbb{R}\} \cup \{\Delta\}$;
- $\text{Dgm}_k(\varphi)$ is the k -th persistence diagram of the continuous function $\varphi: X \rightarrow \mathbb{R}$, and it is a multiset in $\bar{\Delta}^*$, where each of its points has a multiplicity, and, in particular, Δ is a point in $\text{Dgm}_k(\varphi)$ with infinite multiplicity;
- the following function $d: \bar{\Delta}^* \times \bar{\Delta}^* \rightarrow [0, \infty]$ is an extended metric

$$d(p, q) := \begin{cases} C(u, u', v, v') & \text{if } p = (u, v), q = (u', v') \in \Delta^+, \\ |u - u'| & \text{if } p = (u, \infty), q = (u', \infty), \\ \frac{v-u}{2} & \text{if } p = (u, v) \in \Delta^+, = \Delta, \\ \frac{v'-u'}{2} & \text{if } p = \Delta, q = (u', v') \in \Delta^+, \\ 0 & \text{if } p = q = \Delta, \\ \infty & \text{otherwise,} \end{cases}$$

where $C(u, u', v, v') := \min\{\max\{|u - u'|, |v - v'|\}, \max\{\frac{v-u}{2}, \frac{v'-u'}{2}\}\}$;

- if $\varphi = (\varphi_1, \varphi_2): X \rightarrow \mathbb{R}^2$ continuous function, $\varphi_{\mathbf{a}, \mathbf{b}}^* := \min\{a, 1 - a\} \max\{\frac{\varphi_1 - b}{a}, \frac{\varphi_2 + b}{1-a}\}$, with $\mathbf{a} := (a, 1 - a)$, $\mathbf{b} := (b, -b)$, and $a \in]0, 1[$, $b \in \mathbb{R}$.

Let $\varphi, \psi: X \rightarrow \mathbb{R}$ be continuous functions. The k -bottleneck distance [20] is a metric between persistence diagrams defined by

$$d_{B,k}(\varphi, \psi) := d_B(\text{Dgm}_k(\varphi), \text{Dgm}_k(\psi)) = \max_{\sigma} \max_{p \in \text{Dgm}_k(\varphi)} d(p, \sigma(p)),$$

where σ ranges over the multiset bijections between $\text{Dgm}_k(\varphi)$ and $\text{Dgm}_k(\psi)$.

Let $\varphi, \psi: X \rightarrow \mathbb{R}^2$ be continuous functions. The k -th matching distance [16] is a metric between the persistence Betti number functions (rank invariants) defined by

$$d_{\text{match},k}(\varphi, \psi) := \sup_{\mathbf{a}, \mathbf{b}} d_{B,k}(\varphi_{\mathbf{a}, \mathbf{b}}^*, \psi_{\mathbf{a}, \mathbf{b}}^*).$$

Remark 1. Because of the definition of d , the k -bottleneck distance between persistence diagrams $\text{Dgm}_k(\varphi)$ and $\text{Dgm}_k(\psi)$ is of the form $c|w_0 - w_1|$, where $c \in \{\frac{1}{2}, 1\}$, and w_0, w_1 are coordinates of the points of $\text{Dgm}_k(\varphi) \sqcup \text{Dgm}_k(\psi)$.

3 Convex matching distance

Let us consider a continuous function $\varphi = (\varphi_1, \varphi_2): X \rightarrow \mathbb{R}^2$. For every $t \in [0, 1]$, we set $\varphi^t := (1 - t)\varphi_1 + t\varphi_2$.

Definition 1. Considering $\varphi, \psi: X \rightarrow \mathbb{R}^2$ and an integer k , we define the *convex matching distance* cmd_k between φ and ψ as

$$\text{cmd}_k(\varphi, \psi) := \max_{t \in [0, 1]} d_{B,k}(\varphi^t, \psi^t) = \max_{t \in [0, 1]} d_B(\text{Dgm}_k(\varphi^t), \text{Dgm}_k(\psi^t)). \quad (2)$$

Remark 2. We now show that (2) is well defined and that the maximum actually exists. If the function $\varphi = (\varphi_1, \varphi_2)$ is fixed, then for any $t_1, t_2 \in [0, 1]$ we have

$$\begin{aligned} \|\varphi^{t_1} - \varphi^{t_2}\|_{\infty} &= \|(1 - t_1)\varphi_1 + t_1\varphi_2 - ((1 - t_2)\varphi_1 + t_2\varphi_2)\|_{\infty} \\ &= \|\varphi_1 - t_1\varphi_1 + t_1\varphi_2 - \varphi_1 + t_2\varphi_1 - t_2\varphi_2\|_{\infty} \\ &= \|(t_1 - t_2)(\varphi_2 - \varphi_1)\|_{\infty} \\ &= |t_1 - t_2| \|\varphi_1 - \varphi_2\|_{\infty}. \end{aligned}$$

¹Note that these symbols might differ slightly from those used in [26].

It follows that the map $t \mapsto \varphi^t$ is $\|\varphi_1 - \varphi_2\|_\infty$ -Lipschitz. From the stability of the matching distance [16]—which implies $d_{B,k}(\varphi^{t_1}, \varphi^{t_2}) \leq \|\varphi^{t_1} - \varphi^{t_2}\|_\infty$ and $d_{B,k}(\psi^{t_1}, \psi^{t_2}) \leq \|\psi^{t_1} - \psi^{t_2}\|_\infty$ —and by applying the triangle inequality, we get

$$\begin{aligned} \left| d_{B,k}(\varphi^{t_1}, \psi^{t_1}) - d_{B,k}(\varphi^{t_2}, \psi^{t_2}) \right| &\leq d_{B,k}(\varphi^{t_1}, \varphi^{t_2}) + d_{B,k}(\psi^{t_1}, \psi^{t_2}) \\ &\leq \|\varphi^{t_1} - \varphi^{t_2}\|_\infty + \|\psi^{t_1} - \psi^{t_2}\|_\infty \\ &\leq |t_1 - t_2| \|\varphi_1 - \varphi_2\|_\infty + |t_1 - t_2| \|\psi_1 - \psi_2\|_\infty. \end{aligned}$$

It follows that the map $t \mapsto d_{B,k}(\varphi^t, \psi^t)$ is continuous on $[0, 1]$, as claimed.

We also observe that the map $\varphi \mapsto \varphi^t$ is 1-Lipschitz for every $t \in [0, 1]$, since

$$\begin{aligned} \|\varphi^t - \psi^t\|_\infty &= \left\| (1-t)\varphi_1 + t\varphi_2 - ((1-t)\psi_1 + t\psi_2) \right\|_\infty \\ &= \left\| (1-t)(\varphi_1 - \psi_1) + t(\varphi_2 - \psi_2) \right\|_\infty \\ &\leq (1-t)\|\varphi_1 - \psi_1\|_\infty + t\|\varphi_2 - \psi_2\|_\infty \\ &\leq (1-t)\|\varphi - \psi\|_\infty + t\|\varphi - \psi\|_\infty \\ &= \|\varphi - \psi\|_\infty. \end{aligned}$$

Remark 3. If φ is k -times differentiable, with k possibly infinite, then so it is the function φ^t for each $t \in [0, 1]$, due to being defined as the composition of $\varphi = (\varphi_1, \varphi_2)$ with the smooth function $(s_1, s_2) \mapsto (1-t)s_1 + ts_2$. This is a key difference between **cmd** and the classical matching distance, for the operator sending φ to $\varphi_{(a,b)}$ preserves continuity only.

Moreover, the function $t \mapsto \varphi^t$ defined on the interval $[0, 1]$ is smooth (i.e., infinitely differentiable) on $[0, 1]$ (where for the endpoints we mean that the function has continuous left-sided or right-sided derivatives of all required orders). The claim has been already proven for the order 0 in Remark 2. For the other orders, it is enough to notice that, independently from the chosen t , the first derivative of the considered function is $-\varphi_1 + \varphi_2$ while, for higher orders, the derivative is the null function.

Remark 4. We call **cmd** _{k} the *convex matching distance* because it is based on the convex combination of the components of φ and ψ . This idea generalises to the case of functions with values in \mathbb{R}^n : given the function $\varphi = (\varphi_1, \dots, \varphi_n)$, we consider the map assigning to each vector $(t_1, \dots, t_n) \in \mathbb{R}^n$ with $t_i \geq 0$ and $\sum_{i=1}^n t_i = 1$ the function $\varphi^t := \sum_{i=1}^n t_i \varphi_i$.

Proposition 1. **cmd** _{k} is a pseudo-metric.

Proof. It can be easily seen that **cmd** _{k} is a non-negative function, for which the symmetry property and the fact that, for any φ , **cmd** _{k} (φ, φ) = 0 are directly inherited from the bottleneck distance. Thus, to complete the proof, it remains to show that the triangle inequality holds. Since $d_{B,k}$ is a pseudo-metric, for any φ, ψ and ξ we have that

$$\begin{aligned} \mathbf{cmd}_k(\varphi, \psi) &= \max_{t \in [0, 1]} d_{B,k}(\varphi^t, \psi^t) \\ &\leq \max_{t \in [0, 1]} (d_{B,k}(\varphi^t, \xi^t) + d_{B,k}(\xi^t, \psi^t)) \\ &\leq \max_{t \in [0, 1]} d_{B,k}(\varphi^t, \xi^t) + \max_{t \in [0, 1]} d_{B,k}(\xi^t, \psi^t) \\ &= \mathbf{cmd}_k(\varphi, \xi) + \mathbf{cmd}_k(\xi, \psi). \end{aligned}$$

□

Remark 5. We claim that in general **cmd** _{k} is not a metric. Since there exist two real-valued functions f, g such that $f \neq g$ and $d_B(\mathrm{Dgm}_k(f), \mathrm{Dgm}_k(g)) = 0$, we can consider $\varphi = (f, f)$ and $\psi = (g, g)$. Thus, $\varphi^t = f$ and $\psi^t = g$ for any t . Then we obtain that **cmd** _{k} (φ, ψ) = $d_B(\mathrm{Dgm}_k(f), \mathrm{Dgm}_k(g)) = 0$, but $\varphi \neq \psi$.

Proposition 2 (Stability of **cmd** _{k}). *For any k , **cmd** _{k} (φ, ψ) $\leq \|\varphi - \psi\|_\infty$.*

Proof. For any $t \in [0, 1]$, by the stability of the bottleneck distance [20] and Remark 2,

$$d_B(\mathrm{Dgm}_k(\varphi^t), \mathrm{Dgm}_k(\psi^t)) \leq \|\varphi^t - \psi^t\|_\infty \leq \|\varphi - \psi\|_\infty.$$

□

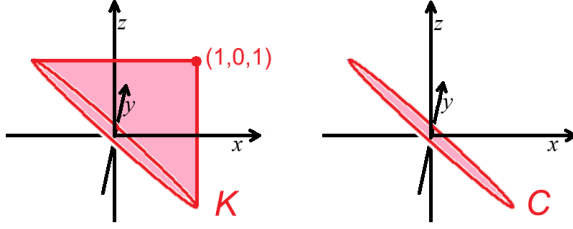


Figure 1: The sets K and C cited in the Examples 1, 2.

4 Comparison with the matching distance

In this section, we compare the newly introduced convex matching distance with the classical matching distance [16].

In Example 1, we exhibit two functions for which the convex matching distance is strictly greater than the classical matching distance, thereby showing that, at least in some cases, the new distance is more discriminative in distinguishing data.

Vice versa, Example 2 provides functions for which the convex matching distance is strictly smaller than the classical matching distance.

Example 1. Let us consider the circumference S in \mathbb{R}^3 of radius $\sqrt{2}$ and center $(0,0,0)$, whose points belong to the plane of equation $x+z=0$. Then, let us consider the circle C bounded by S and the conical set K obtained by taking the union of the segments joining the point $(1,0,1)$ to each point of S (see Figure 1). We set $\varphi(x,y,z) := (x,z)$ for $(x,y,z) \in K$ and $\psi(x,y,z) := (x,z)$ for $(x,y,z) \in C$. Given that K and C are homeomorphic to the closed hemisphere $\Sigma := \{(x,y,z) \in \mathbb{R}^3 : x^2 + y^2 + z^2 = 1, x+z \geq 0\}$, we can find two homeomorphisms $\mathbf{h}_K : \Sigma \rightarrow K$, $\mathbf{h}_C : \Sigma \rightarrow C$. Therefore, we can consider the continuous functions $\hat{\varphi} : \Sigma \rightarrow \mathbb{R}^2$, $\hat{\varphi} := \varphi \circ \mathbf{h}_K$, $\hat{\psi} : \Sigma \rightarrow \mathbb{R}^2$, $\hat{\psi} := \psi \circ \mathbf{h}_C$. Let us now compute the following persistence diagrams in degree 1:

$$\begin{aligned} \text{Dgm}_1(\hat{\varphi}_{\mathbf{a},\mathbf{b}}^*) &= \text{Dgm}_1(\varphi_{\mathbf{a},\mathbf{b}}^*) = \{\Delta\} = \text{Dgm}_1(\psi_{\mathbf{a},\mathbf{b}}^*) = \text{Dgm}_1(\hat{\psi}_{\mathbf{a},\mathbf{b}}^*) \text{ for any } \mathbf{a}, \mathbf{b}; \\ \text{Dgm}_1\left(\hat{\varphi}^{\frac{1}{2}}\right) &= \text{Dgm}_1\left(\varphi^{\frac{1}{2}}\right) = \{\Delta, (0,1)\} \text{ and } \text{Dgm}_1\left(\hat{\psi}^{\frac{1}{2}}\right) = \text{Dgm}_1\left(\psi^{\frac{1}{2}}\right) = \{\Delta\}. \end{aligned}$$

Therefore, $d_{\text{match},1}(\hat{\varphi}, \hat{\psi}) = 0$ and $d_B\left(\hat{\varphi}^{\frac{1}{2}}, \hat{\psi}^{\frac{1}{2}}\right) = \frac{1}{2}$. Hence $\text{cmd}_1(\hat{\varphi}, \hat{\psi}) \geq \frac{1}{2} > 0 = d_{\text{match},1}(\hat{\varphi}, \hat{\psi})$.

However, the convex matching distance is not always greater than the classical matching distance, as shown by the following example.

Example 2. If we consider degree 0 instead of degree 1, the functions given in Example 1 show a case in which the convex matching distance is strictly smaller than the classical matching distance. In fact, it is easy to verify that

$$\begin{aligned} \text{Dgm}_0\left(\hat{\varphi}_{(\frac{1}{2},\frac{1}{2}),(0,0)}^*\right) &= \text{Dgm}_0\left(\varphi_{(\frac{1}{2},\frac{1}{2}),(0,0)}^*\right) = \{\Delta, (0,1), (0,\infty)\}; \\ \text{Dgm}_0\left(\hat{\psi}_{(\frac{1}{2},\frac{1}{2}),(0,0)}^*\right) &= \text{Dgm}_0\left(\psi_{(\frac{1}{2},\frac{1}{2}),(0,0)}^*\right) = \{\Delta, (0,\infty)\}; \\ \text{Dgm}_0(\hat{\varphi}^t) &= \text{Dgm}_0(\varphi^t) = \{\Delta, (1-2t, \infty)\} = \text{Dgm}_0(\psi^t) = \text{Dgm}_0(\hat{\psi}^t) \text{ for any } t \in [0,1]. \end{aligned}$$

Therefore, $d_{\text{match},0}(\hat{\varphi}, \hat{\psi}) \geq \frac{1}{2}$ and $d_B(\text{Dgm}_0(\varphi^t), \text{Dgm}_0(\psi^t)) = 0$ for any $t \in [0,1]$. Hence, $\text{cmd}_0(\hat{\varphi}, \hat{\psi}) = 0 < \frac{1}{2} \leq d_{\text{match},0}(\hat{\varphi}, \hat{\psi})$.

Remark 6. The above examples can be suitably modified to satisfy more restrictive conditions on the smoothness of the involved functions or on their domains, taken to be manifolds. This shows that their existence is not due to a lack of regularity properties but rather follows from the very definition of the two distances. By identifying the boundaries of two disjoint copies of K and C , respectively, the above examples can be adapted, thus obtaining two smooth functions $\tilde{\varphi}, \tilde{\psi} : \mathbb{S}^2 \rightarrow \mathbb{R}^2$ such that:

- $d_{\text{match},1}(\tilde{\varphi}, \tilde{\psi}) = 0 < \frac{1}{2} \leq \text{cmd}_1(\tilde{\varphi}, \tilde{\psi})$;
- $\text{cmd}_0(\tilde{\varphi}, \tilde{\psi}) = 0 < \frac{1}{2} \leq d_{\text{match},0}(\tilde{\varphi}, \tilde{\psi})$.

5 Pareto grid and Position Theorem

Let M be a closed (i.e., compact and without boundary) smooth Riemannian manifold of dimension $r \geq 2$ and $\varphi = (\varphi_1, \varphi_2): M \rightarrow \mathbb{R}^2$ a smooth function.

Definition 2.

1. The *Jacobi set*, $\mathbb{J}(\varphi)$, is the set of all points $x \in M$ at which the gradients of φ_1 and φ_2 are linearly dependent, namely $x \in \mathbb{J}(\varphi)$ if and only if there exists $(\lambda_1, \lambda_2) \neq (0, 0)$ such that $\lambda_1 \nabla \varphi_1(x) + \lambda_2 \nabla \varphi_2(x) = 0$.
2. The *Pareto critical set* of φ , $\mathbb{J}_P(\varphi)$, is the set of all points $x \in \mathbb{J}(\varphi)$ such that there exists $(\lambda_1, \lambda_2) \neq (0, 0)$ with $\lambda_1, \lambda_2 \geq 0$ such that $\lambda_1 \nabla \varphi_1(x) + \lambda_2 \nabla \varphi_2(x) = 0$. The elements of $\mathbb{J}_P(\varphi)$ are called *Pareto critical points*. Note that $\mathbb{J}_P(\varphi)$ contains both the critical points of φ_1 and those of φ_2 .

Unless otherwise specified, throughout the rest of the article the smooth functions considered will satisfy the following conditions.

Assumption 1.

1. No point x exists in M at which both $\nabla \varphi_1(x)$ and $\nabla \varphi_2(x)$ vanish.
2. $\mathbb{J}(\varphi)$ is a 1-dimensional manifold smoothly embedded in M , consisting of finitely many components, each diffeomorphic to a circle.
3. $\mathbb{J}_P(\varphi)$ is a 1-dimensional closed submanifold of $\mathbb{J}(\varphi)$ with boundary.
4. The connected components of $\mathbb{J}_P(\varphi) \setminus \mathbb{J}_C(\varphi)$ are finite in number, each being diffeomorphic to an interval, where $\mathbb{J}_C(\varphi)$ is the set of cusp points of φ , i.e., the set of points of $\mathbb{J}(\varphi)$ at which the restriction of φ to $\mathbb{J}(\varphi)$ fails to be an immersion. In other words, $\mathbb{J}_C(\varphi)$ is the subset of $\mathbb{J}(\varphi)$ where both $\nabla \varphi_1$ and $\nabla \varphi_2$ are orthogonal to $\mathbb{J}(\varphi)$. With respect to any parameterisation of each component, one of φ_1 and φ_2 is strictly increasing and the other is strictly decreasing. Each component may meet critical points of φ_1 or φ_2 only at its endpoints.

We call the closures of the images of the connected components of $\mathbb{J}_P(\varphi) \setminus \mathbb{J}_C(\varphi)$ (proper) *contours* [17], and denote by $\text{Ctr}(\varphi)$ the set of contours of φ . Given two smooth functions $\varphi, \psi: M \rightarrow \mathbb{R}^2$, we set $\text{Ctr}(\varphi, \psi) := \text{Ctr}(\varphi) \cup \text{Ctr}(\psi)$. It is important to observe that Assumption 1 is generic within the class of smooth functions from M to \mathbb{R}^2 [34].

In our setting, we make one further technical assumption.

Assumption 2.

1. The set $\mathbb{J}_C(\varphi)$ of cusp points is empty.
2. Each contour $\alpha \in \text{Ctr}(\varphi)$ is a smooth regular curve in $\mathcal{C}^\infty([0, 1]; \mathbb{R}^2)$.

Definition 3. The *Pareto grid* of φ is the subset of \mathbb{R}^2 defined as the image $\varphi(\mathbb{J}_P(\varphi))$.

Figure 2 shows the Pareto grid of the projection of a 2-sphere in \mathbb{R}^2 .

Before presenting the main result of this section, we recall the following well-established theorem, which provides a useful relation between the persistence diagram of a smooth function and its critical values. This statement is a technical but standard fact in the literature, and we include it here without proof (cf., e.g., Theorem 3.1 in [32], and [24]).

Theorem 1. Let M be a closed smooth manifold and $\varphi: M \rightarrow \mathbb{R}$ a smooth function. If w is a finite coordinate of a point $p \in \text{Dgm}_k(\varphi) \setminus \{\Delta\}$, then w is a critical value for φ .

We are now ready to state the main result of this section. Relying on Theorem 1, it provides a geometric characterisation of the points in the persistence diagram of φ^t in terms of the contours associated with φ . Next theorem is analogous to [17, Theorem 2]. In what follows, the symbol \cdot denotes the dot product.

Theorem 2 (Position Theorem for φ^t). *Let $t \in [0, 1]$ and let w be a finite coordinate of a point in $\text{Dgm}_k(\varphi^t) \setminus \{\Delta\}$. Then there exist a contour denoted as $\alpha = (\alpha_1, \alpha_2): [0, 1] \rightarrow \mathbb{R}^2$ and a $\bar{t} \in [0, 1]$ such that:*

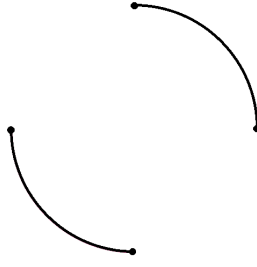


Figure 2: The Pareto grid of the function $\varphi : \mathbb{S}^2 \rightarrow \mathbb{R}^2$ defined by setting $\varphi(x, y, z) := (x, z)$.

$$1. \quad \boldsymbol{\alpha}(\bar{\tau}) \cdot (1-t, t) = w;$$

$$2. \quad \frac{d\boldsymbol{\alpha}}{d\tau}(\bar{\tau}) \cdot (1-t, t) = 0.$$

Proof. By Theorem 1 we know that w must be a critical value for φ^t . Therefore, there exists a point $\bar{x} \in M$ such that $w = \varphi^t(\bar{x})$ and $\nabla \varphi^t(\bar{x}) = \mathbf{0}$, where $\mathbf{0}$ denotes the null vector. Hence, $(1-t)\nabla \varphi_1(\bar{x}) + t\nabla \varphi_2(\bar{x}) = \mathbf{0}$. This means that \bar{x} is a Pareto critical point of φ . Therefore, there exist a contour $\boldsymbol{\alpha} = (\alpha_1, \alpha_2) : [0, 1] \rightarrow \mathbb{R}^2$ and a $\bar{\tau} \in [0, 1]$ such that $\varphi(\bar{x}) = \boldsymbol{\alpha}(\bar{\tau})$, and

$$w = \varphi^t(\bar{x}) = (1-t)\varphi_1(\bar{x}) + t\varphi_2(\bar{x}) = \varphi(\bar{x}) \cdot (1-t, t) = \boldsymbol{\alpha}(\bar{\tau}) \cdot (1-t, t).$$

Consider a smooth regular curve $\gamma : [0, 1] \rightarrow M$ such that $\boldsymbol{\alpha}(\tau) = \varphi \circ \gamma(\tau)$ and $\gamma(\bar{\tau}) = \bar{x}$, which implies that $\boldsymbol{\alpha}(\bar{\tau}) = (\alpha_1(\bar{\tau}), \alpha_2(\bar{\tau})) = (\varphi_1(\gamma(\bar{\tau})), \varphi_2(\gamma(\bar{\tau}))) = (\varphi_1(\bar{x}), \varphi_2(\bar{x}))$. By Assumption 2, $\mathbb{J}_C(\varphi)$ is empty, hence $\frac{d}{d\tau}(\varphi \circ \gamma(\tau))$ does not vanish for any $\tau \in [0, 1]$. Therefore, we have that

$$\begin{aligned}
0 &= \mathbf{0} \cdot \frac{d\gamma}{d\tau}(\bar{\tau}) \\
&= \nabla \varphi^t(\bar{x}) \cdot \frac{d\gamma}{d\tau}(\bar{\tau}) \\
&= ((1-t)\nabla \varphi_1(\bar{x}) + t\nabla \varphi_2(\bar{x})) \cdot \frac{d\gamma}{d\tau}(\bar{\tau}) \\
&= (1-t)\nabla \varphi_1(\bar{x}) \cdot \frac{d\gamma}{d\tau}(\bar{\tau}) + t\nabla \varphi_2(\bar{x}) \cdot \frac{d\gamma}{d\tau}(\bar{\tau}) \\
&= (1-t)\frac{d\varphi_1 \circ \gamma}{d\tau}(\bar{\tau}) + t\frac{d\varphi_2 \circ \gamma}{d\tau}(\bar{\tau}) \\
&= (1-t)\frac{d\alpha_1}{d\tau}(\bar{\tau}) + t\frac{d\alpha_2}{d\tau}(\bar{\tau}) \\
&= \frac{d\boldsymbol{\alpha}}{d\tau}(\bar{\tau}) \cdot (1-t, t).
\end{aligned} \tag{3}$$

□

It may be useful here to observe how the Position Theorem 2 can be used to find the finite coordinates of the points in $\text{Dgm}_k(\varphi^t) \setminus \{\Delta\}$. The idea is to consider the family of parallel lines having the direction of the vector $(1-t, t)$ and to look for the points where these lines intersect the contours associated with the function $\varphi : M \rightarrow \mathbb{R}^2$ orthogonally. For each such point P , one computes the scalar product $P \cdot (1-t, t)$. As P varies, one thus obtains all the finite coordinates of the points in $\text{Dgm}_k(\varphi^t) \setminus \{\Delta\}$.

6 Special values

For the following definitions we need to introduce the notion of signed radius:

Definition 4. Let $\boldsymbol{\alpha}$ be a regular smooth curve in \mathbb{R}^2 and let $P \in \boldsymbol{\alpha}$. If the curvature of $\boldsymbol{\alpha}$ at P is non-zero, let (x, y) and ρ denote the centre and radius of the osculating circle to $\boldsymbol{\alpha}$ at P , and define the *signed radius* of $\boldsymbol{\alpha}$ at P as $\ell = \text{sign}((P - (x, y)) \cdot (1, 0))\rho$.

Definition 5. The *special set* of (φ, ψ) , denoted by $\text{Sp}(\varphi, \psi)$, consists of the values $t \in [0, 1]$ such that at least one of the following hold:

1. There exists a line r with direction $(1 - t, t)$ intersecting orthogonally a contour $\alpha \in \text{Ctr}(\varphi, \psi)$ at one of its endpoints.
2. There exist lines r_1, r_2, r_3, r_4 with direction $(1 - t, t)$ and contours $\alpha_1, \alpha_2, \alpha_3, \alpha_4 \in \text{Ctr}(\varphi, \psi)$ such that r_i intersects α_i orthogonally at P_i , for each $i \in \{1, 2, 3, 4\}$, with $\{P_1, P_2\} \neq \{P_3, P_4\}$, and $(P_1 - P_2) \cdot (1 - t, t) = c((P_3 - P_4) \cdot (1 - t, t))$, for $c \in \{\frac{1}{2}, 1\}$.
3. There exist lines r_1, r_2 with direction $(1 - t, t)$ and contours $\alpha_1, \alpha_2 \in \text{Ctr}(\varphi, \psi)$ such that r_i intersects the interior of α_i orthogonally at P_i , for i in $\{1, 2\}$, with $P_1 \neq P_2$ and one of the following conditions holds:
 - α_1 has null curvature at P_1 ,
 - α_2 has null curvature at P_2 ,
 - ℓ_1 and ℓ_2 are defined and $\ell_1 = \ell_2$,
 - ℓ_1 and ℓ_2 are defined, with $\ell_1 \neq \ell_2$, and

$$t = \frac{\zeta}{1 + \zeta} \text{ with } \zeta := \tan \left(\frac{1}{2} \arcsin \left(1 - \left(\frac{(y_1 - y_2) - (x_1 - x_2)}{(\ell_1 - \ell_2)} \right)^2 \right) \right),$$

where ℓ_i is the signed radius and (x_i, y_i) is the center of the osculating circle of α_i at P_i , for i in $\{1, 2\}$.

Remark 7. Note that $t = 0$ and $t = 1$ are always special values for each φ, ψ . For example, to see that $t = 0$ is special, let x in M be a point at which φ_1 attains its maximum. Then $\varphi(x)$ is the endpoint of some contour $\alpha \in \text{Ctr}(\varphi)$. In particular, let $\gamma: [0, 1] \rightarrow M$ be such that $\alpha(\tau) = \varphi \circ \gamma(\tau)$ and suppose that $\gamma(0) = x$. Therefore,

$$0 = \nabla \varphi_1(x) \cdot \frac{d\gamma}{d\tau}(0) = \frac{d(\varphi_1 \circ \gamma)}{d\tau}(0) = \frac{d\alpha_1}{d\tau}(0) = \frac{d\alpha}{d\tau}(0) \cdot (1, 0).$$

Hence $(1, 0)$ is orthogonal to α at an endpoint. One shows in an analogous way that $t = 1$ is also a special value.

Remark 8. The intuition behind Definition 5.2 is the following: if $t \in [0, 1]$ satisfies Definition 5.2, then t is a value at which the optimal matching between $\text{Dgm}(\varphi^t)$ and $\text{Dgm}(\psi^t)$ may change abruptly. In particular, if σ is such an optimal matching and $p_1, p_2, p_3, p_4 \in \text{Dgm}(\varphi^t) \cup \text{Dgm}(\psi^t)$ are such that $\text{cost } \sigma = w_1 - w_2 = c(w_3 - w_4)$, where w_i is a finite coordinate of p_i , $i = 1, \dots, 4$, then, in a neighbourhood of t , the optimal matching could be either the one matching p_1 to p_2 or the one matching p_3 to p_4 , but not the other. A similar motivation led to the definition of special set in [23], relatively to the classical matching distance.

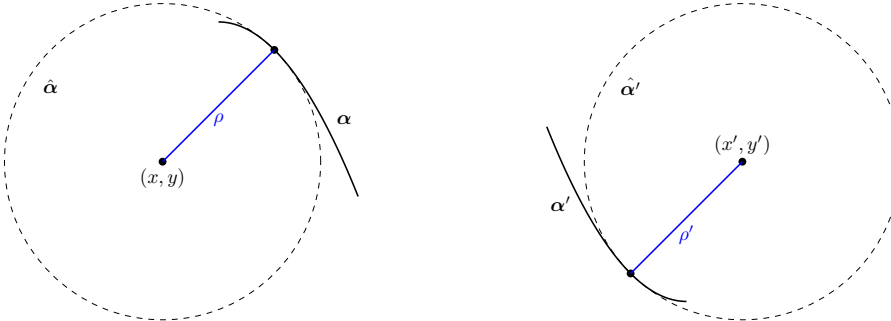


Figure 3: Osculating circles $\hat{\alpha}$ and $\hat{\alpha}'$ of centres $(x, y), (x', y')$ and radii ρ, ρ' to a negative and positive parabola denoted by α and α' , respectively, at a non-critical point. The signed radius ℓ from Definition 4 is positive on the leftmost case and negative on the rightmost one.

Remark 9. We note that the radius ℓ^i appearing in Definition 5.3 has positive sign whenever P_i is above and to the right of the centre of the osculating circle, and negative when it is below and on the left. These are the only cases possible due to Assumption 1.4, which are illustrated in Figure 3.

The next result characterises the values of t at which the convex matching distance is attained. These values always exist by Remark 2. We observe that when the convex matching distance is zero, every $t \in [0, 1]$ realises it.

Theorem 3. *If $\mathbf{cmd}_k(\varphi, \psi) > 0$ and it is realised at \bar{t} , that is,*

$$\mathbf{cmd}_k(\varphi, \psi) = d_{B,k}(\varphi^{\bar{t}}, \psi^{\bar{t}}),$$

then $\bar{t} \in \text{Sp}(\varphi, \psi)$.

Proof. By contradiction, suppose $\bar{t} \notin \text{Sp}(\varphi, \psi)$ and $\mathbf{cmd}_k(\varphi, \psi) = d_{B,k}(\varphi^{\bar{t}}, \psi^{\bar{t}})$.

By Remark 1 there exist coordinates $w_0, w_1 \in \mathbb{R}$ of points in $\text{Dgm}_k(\varphi^{\bar{t}}) \cup \text{Dgm}_k(\psi^{\bar{t}})$ and a constant $c \in \{\frac{1}{2}, 1\}$ such that $\mathbf{cmd}_k(\varphi, \psi) = c|w_0 - w_1| > 0$. Moreover, by Theorem 2, there exist two contours $\alpha, \beta \in \text{Ctr}(\varphi, \psi)$ such that, for some τ_α and τ_β in $[0, 1]$:

$$\begin{aligned} \alpha(\tau_\alpha) \cdot (1 - \bar{t}, \bar{t}) &= w_0, \\ \beta(\tau_\beta) \cdot (1 - \bar{t}, \bar{t}) &= w_1, \end{aligned}$$

where with a slight abuse of notation we denote with $\alpha(\tau), \beta(\tau')$ some smooth parametrisations of α and β such that $(1 - \bar{t}, \bar{t})$ is orthogonal to α and β at $\alpha(\tau_\alpha)$ and $\beta(\tau_\beta)$, respectively. By Definition 5.2 no two distinct pairs of coordinates can realise $d_{B,k}(\varphi^{\bar{t}}, \psi^{\bar{t}})$, hence $\{w_0, w_1\}$ is unique. Moreover, note that τ_α and τ_β cannot be in $\{0, 1\}$, since 0 and 1 are special values (see Remark 7), it is enough to consider the interior of the contours α and β .

Now, we locally reparametrise the interior of the contours α and β in neighborhoods of $\alpha(\tau_\alpha)$ and $\beta(\tau_\beta)$, respectively. Let $\theta(t) := \arctan\left(\frac{t}{1-t}\right) \in]0, \frac{\pi}{2}[$ for $t \in]0, 1[$ and let $\bar{\theta} := \theta(\bar{t})$. Consider the osculating circles $\hat{\alpha}$ and $\hat{\beta}$ at $\alpha(\tau_\alpha)$ and $\beta(\tau_\beta)$, which may be parametrised as $\hat{\alpha}(\theta) := (x_\alpha, y_\alpha) + \ell_\alpha(\cos \theta, \sin \theta)$ and $\hat{\beta}(\theta) := (x_\beta, y_\beta) + \ell_\beta(\cos \theta, \sin \theta)$, where ℓ_α, ℓ_β and $(x_\alpha, y_\alpha), (x_\beta, y_\beta)$ denote the signed radii – in the sense of Definition 4 – and centres of the osculating circles, and the parameter θ varies in $[0, 2\pi[$. Note that, $\hat{\alpha}(\bar{\theta}) = \alpha(\tau_\alpha)$. Moreover, by Definition 5.3 and Assumption 2, we have $|\ell_\alpha|, |\ell_\beta| \in]0, \infty[$. Consider the line $r(\theta) := \{(x_\alpha, y_\alpha) + s(\cos \theta, \sin \theta) \mid s \in \mathbb{R}\}$, and let $\alpha(\theta)$ be the local and smooth parametrisation of α given by the intersection $\alpha \cap r(\theta)$ in a neighbourhood of $\bar{\theta}$. The existence of this parametrisation is by the transversality between α and $r(\theta)$ provided by Assumption 1.

By reparametrising β in a neighborhood of $\beta(\tau_\beta)$ in the same fashion, we obtain $\beta(\bar{\theta}) = \beta(\tau_\beta)$. Thus, we can consider the difference $w_0(\theta) - w_1(\theta) = \alpha(\theta) \cdot (1 - t, t) - \beta(\theta) \cdot (1 - t, t)$. To finish the proof we will show that $\dot{w}_0(\bar{\theta}) - \dot{w}_1(\bar{\theta}) \neq 0$, where we denote with the upper dot the derivative with respect to θ .

By definition of θ and osculating circles, we have $\alpha(\bar{\theta}) = \hat{\alpha}(\bar{\theta}), \beta(\bar{\theta}) = \hat{\beta}(\bar{\theta}), \dot{\alpha}(\bar{\theta}) = \dot{\hat{\alpha}}(\bar{\theta})$ and $\dot{\beta}(\bar{\theta}) = \dot{\hat{\beta}}(\bar{\theta})$. Noting that $(1 - t, t) = \left(\frac{\cos \theta}{\cos \theta + \sin \theta}, \frac{\sin \theta}{\cos \theta + \sin \theta}\right)$, we can explicitly compute the derivative $\dot{w}_0(\theta)$ in a neighborhood of $\bar{\theta}$:

$$\begin{aligned} \dot{w}_0(\theta) &= \frac{\partial}{\partial \theta} \left[\alpha(\theta) \cdot \left(\frac{\cos \theta}{\cos \theta + \sin \theta}, \frac{\sin \theta}{\cos \theta + \sin \theta} \right) \right] \\ &= \dot{\alpha}(\theta) \cdot \left(\frac{\cos \theta}{\cos \theta + \sin \theta}, \frac{\sin \theta}{\cos \theta + \sin \theta} \right) + \alpha(\theta) \cdot \frac{(-1, 1)}{(\cos \theta + \sin \theta)^2}. \end{aligned} \tag{4}$$

The denominators in the previous expression do not vanish since $\theta \in]0, \frac{\pi}{2}[$. As $\dot{\alpha}(\bar{\theta}) = \dot{\hat{\alpha}}(\bar{\theta})$, we can rewrite (4) using the parametrisation of the osculating circle $\hat{\alpha}$:

$$\begin{aligned} \dot{w}_0(\bar{\theta}) &= \left[\ell_\alpha(-\sin \theta, \cos \theta) \cdot \left(\frac{\cos \theta}{\cos \theta + \sin \theta}, \frac{\sin \theta}{\cos \theta + \sin \theta} \right) \right. \\ &\quad \left. + ((x_\alpha, y_\alpha) + \ell_\alpha(\cos \theta, \sin \theta)) \cdot \frac{(-1, 1)}{(\cos \theta + \sin \theta)^2} \right]_{\theta=\bar{\theta}} \\ &= \left[\frac{y_\alpha - x_\alpha + \ell_\alpha(\sin \theta - \cos \theta)}{(\cos \theta + \sin \theta)^2} \right]_{\theta=\bar{\theta}}. \end{aligned} \tag{5}$$

By using the osculating circle $\hat{\beta}$ we can replicate the same reasoning to compute $\dot{w}_1(\bar{\theta})$. Subtracting both formulas we obtain:

$$\frac{d}{d\theta} [w_0(\theta) - w_1(\theta)]_{\theta=\bar{\theta}} = 0 \quad \text{if and only if} \quad \cos \bar{\theta} - \sin \bar{\theta} = \frac{(y_\alpha - y_\beta) - (x_\alpha - x_\beta)}{\ell_\alpha - \ell_\beta}, \tag{6}$$

where the radii ℓ_α, ℓ_β have positive or negative sign according to Definition 4.

Note that the denominator on the right-hand side of (6) does not vanish by Definition 5.3. Recall the trigonometric formula $(\cos \theta - \sin \theta)^2 = 1 - \sin 2\theta$, which applied to (6) yields

$$\bar{\theta} = \frac{1}{2} \arcsin \left(1 - \left(\frac{(y_\alpha - y_\beta) - (x_\alpha - x_\beta)}{\rho_\alpha - \rho_\beta} \right)^2 \right).$$

Lastly, applying back the change of variables $\tan \theta = \frac{t}{1-t}$ to the left-hand side of the last equation with $t = \bar{t}$ yields exactly the condition in Definition 5.3, implying $\bar{t} \in \text{Sp}(\varphi, \psi)$. This generates the desired contradiction. \square

Remark 10. In the proof of Theorem 3, we use the fact that the parametrisation of α defined by the intersection $\alpha \cap r(\theta)$ is smooth in a neighborhood of $\alpha(\tau_\alpha)$. The fact that $\alpha(\theta)$ is a well-defined and smooth curve follows from the assumption that all lines passing through the point (x_α, y_α) intersect the contour α transversally.

7 Conclusions

In this work, we introduced the convex matching distance, a new pseudo-metric to compare functions with values in \mathbb{R}^2 . If φ and ψ are two such functions, the convex matching distance is defined by maximising the bottleneck distance between the persistence diagrams of the convex combinations φ^t and ψ^t of the coordinates of φ and ψ . Whereas the classical matching distance requires the computation of a two-parameter family of persistence diagrams (see [16, 2, 26]), our metric depends only on the one-parameter family indexed by $t \in [0, 1]$. This reduction in dimensionality, combined with the additional regularity of the operator sending φ to φ^t , leads to both conceptual simplifications and computational advantages improving the effective computability of the metric. Moreover, the smoothness preservation property of the proposed operator allows for its incorporation into learning-based frameworks, ensuring stable and well-behaved gradients and enabling the use of standard optimization and training procedures.

Under generic regularity assumptions on the input functions, we show in Theorem 3 that the convex matching distance is realised at some parameter in a distinguished subset of $[0, 1]$, that we called special set. We conjecture that this subset is finite under generic conditions on the input pair (φ, ψ) . It is not hard to find examples of pairs of functions having an infinite special set. For example, this happens when $\text{Ctr}(\varphi, \psi)$ contains two contours such that one is the translated of the other, or when a contour has zero curvature. However, in our opinion, these phenomena occur when the pair of functions is not generic, as the functions can be infinitesimally modified locally, so not to have this properties any more.

Future work will focus on the effective computation of the parameters belonging to this special set as well as on the identification of the proper genericity assumptions under which such a set is finite. Moreover, we aim to weaken the assumptions under which we proved Theorem 3 and to prove their genericity.

Finally, as mentioned in the introduction the operator that given a parameter t maps each function φ to the function φ^t is just one of the infinitely many possibilities for assigning a parametric family of functions to φ . In the near future, we intend to investigate alternative operators and evaluate the advantages and drawbacks associated with their adoption.

Acknowledgements

P.F. was supported by GNSAGA-INDAM, CNIT National Laboratory WiLab, and the WiLab-Huawei Joint Innovation Center. U.F. acknowledges the Italian National Biodiversity Future Center (NBFC) - National Recovery and Resilience Plan (NRRP) funded by the EU-NextGenerationEU (project code CN 00000033) and the Innovation Ecosystem Robotics and AI for Socio-economic Empowerment (RAISE) - National Recovery and Resilience Plan (NRRP) funded by the EU-NextGenerationEU (project code ECS 00000035). E.M.G. was supported by GNAMPA-INDAM and GNAMPA Project CUP E53C22001930001. N.Q. was supported by CNIT National Laboratory WiLab, and the WiLab-Huawei Joint Innovation Center. S.S. acknowledges the GNSAGA-INDAM and the MUR Excellence Department Project MatMod@TOV awarded to the Department of Mathematics, University of Rome Tor Vergata, CUP E83C23000330006. F.T. was funded by the Knut and Alice Wallenberg Foundations and the WASP Postdoctoral Scholarship Program.

References

- [1] Majid Allili, Tomasz Kaczynski, and Claudia Landi. Reducing complexes in multidimensional persistent homology theory. *J. Symbolic Comput.*, 78:61–75, 2017. doi:10.1016/j.jsc.2015.11.020.
- [2] Asilata Bapat, Robyn Brooks, Celia Hacker, Claudia Landi, Barbara I. Mahler, and Elizabeth R. Stephenson. Computing the matching distance of 2-parameter persistence modules from critical values. *arXiv e-prints*, October 2022. doi:10.48550/arXiv.2210.12868.
- [3] Mattia G Bergomi, Patrizio Frosini, Daniela Giorgi, and Nicola Quicioli. Towards a topological–geometrical theory of group equivariant non-expansive operators for data analysis and machine learning. *Nature Machine Intelligence*, 1(9):423–433, 2019.
- [4] S. Biasotti, A. Cerri, P. Frosini, D. Giorgi, and C. Landi. Multidimensional size functions for shape comparison. *J. Math. Imaging Vision*, 32(2):161–179, 2008. doi:10.1007/s10851-008-0096-z.
- [5] Silvia Biasotti, Andrea Cerri, Patrizio Frosini, and Daniela Giorgi. A new algorithm for computing the 2-dimensional matching distance between size functions. *Pattern Recognition Letters*, 32(14):1735–1746, 2011. doi:10.1016/j.patrec.2011.07.014.
- [6] Håvard Bakke Bjerkevik and Michael Kerber. Asymptotic improvements on the exact matching distance for 2-parameter persistence. *J. Comput. Geom.*, 14(1):309–342, 2023. doi:10.3982/qe2088.
- [7] Giovanni Bocchi, Stefano Botteghi, Martina Brasini, Patrizio Frosini, and Nicola Quicioli. On the finite representation of linear group equivariant operators via permutant measures. *Annals of Mathematics and Artificial Intelligence*, 91:1–23, 02 2023. doi:10.1007/s10472-022-09830-1.
- [8] Giovanni Bocchi, Massimo Ferri, and Patrizio Frosini. A novel approach to graph distinction through GENEOs and permutants. *Scientific Reports*, 15(1):6259, Feb 2025. doi:10.1038/s41598-025-90152-7.
- [9] Giovanni Bocchi, Patrizio Frosini, Alessandra Micheletti, Alessandro Pedretti, Gianluca Palermo, Davide Gadioli, Carmen Gratteri, Filippo Lunghini, Akash Deep Biswas, Pieter F. W. Stouten, Andrea R. Beccari, Anna Fava, and Carmine Talarico. Geneonet: a breakthrough in protein binding pocket detection using group equivariant non-expansive operators. *Scientific Reports*, 15(1):34597, Oct 2025. doi:10.1038/s41598-025-18132-5.
- [10] Francesca Cagliari, Barbara Di Fabio, and Massimo Ferri. One-dimensional reduction of multidimensional persistent homology. *Proc. Amer. Math. Soc.*, 138(8):3003–3017, 2010. doi:10.1090/S0002-9939-10-10312-8.
- [11] Francesca Cagliari and Claudia Landi. Finiteness of rank invariants of multidimensional persistent homology groups. *Appl. Math. Lett.*, 24(4):516–518, 2011. doi:10.1016/j.aml.2010.11.004.
- [12] Gunnar Carlsson, Gurjeet Singh, and Afra Zomorodian. Computing multidimensional persistence. *J. Comput. Geom.*, 1(1):72–100, 2010. doi:10.20382/jocg.v1i1a6.
- [13] Gunnar Carlsson and Afra Zomorodian. The theory of multidimensional persistence. *Discrete Comput. Geom.*, 42(1):71–93, 2009. doi:10.1007/s00454-009-9176-0.
- [14] N. Cavazza, M. Ethier, P. Frosini, T. Kaczynski, and C. Landi. Comparison of persistent homologies for vector functions: from continuous to discrete and back. *Comput. Math. Appl.*, 66(4):560–573, 2013. doi:10.1016/j.camwa.2013.06.004.
- [15] Niccolò Cavazza, Massimo Ferri, and Claudia Landi. Estimating multidimensional persistent homology through a finite sampling. *International Journal of Computational Geometry & Applications*, 25(03):187–205, 2015. doi:10.1142/S0218195915500119.
- [16] Andrea Cerri, Barbara Di Fabio, Massimo Ferri, Patrizio Frosini, and Claudia Landi. Betti numbers in multidimensional persistent homology are stable functions. *Mathematical Methods in the Applied Sciences*, 36(12):1543–1557, 2013. doi:10.1002/mma.2704.

[17] Andrea Cerri, Marc Ethier, and Patrizio Frosini. On the geometrical properties of the coherent matching distance in 2D persistent homology. *J. Appl. Comput. Topol.*, 3(4):381–422, 2019. doi:10.1007/s41468-019-00041-y.

[18] Andrea Cerri and Patrizio Frosini. Necessary conditions for discontinuities of multidimensional persistent Betti numbers. *Mathematical Methods in the Applied Sciences*, 38(4):617–629, 2015. doi:10.1002/mma.3093.

[19] Andrea Cerri and Claudia Landi. The persistence space in multidimensional persistent homology. In Rocio Gonzalez-Diaz, Maria-Jose Jimenez, and Belen Medrano, editors, *Discrete Geometry for Computer Imagery*, pages 180–191, Berlin, Heidelberg, 2013. Springer Berlin Heidelberg.

[20] David Cohen-Steiner, Herbert Edelsbrunner, and John Harer. Stability of persistence diagrams. *Discrete & Computational Geometry*, 37(1):103–120, Jan 2007. doi:10.1007/s00454-006-1276-5.

[21] Jacopo Joy Colombini, Filippo Bonchi, Francesco Giannini, Fosca Giannotti, Roberto Pellungrini, and Patrizio Frosini. Mathematical foundation of interpretable equivariant surrogate models. In Riccardo Guidotti, Ute Schmid, and Luca Longo, editors, *Explainable Artificial Intelligence*, pages 294–318, Cham, 2026. Springer Nature Switzerland.

[22] Michele d’Amico, Patrizio Frosini, and Claudia Landi. Natural pseudo-distance and optimal matching between reduced size functions. *Acta Applicandae Mathematicae*, 109(2):527–554, Feb 2010. doi:10.1007/s10440-008-9332-1.

[23] Marc Ethier, Patrizio Frosini, Nicola Quercioli, and Francesca Tombari. Geometry of the matching distance for 2D filtering functions. *Journal of Applied and Computational Topology*, 7(4):815–830, Dec 2023. doi:10.1007/s41468-023-00128-7.

[24] Patrizio Frosini. Connections between size functions and critical points. *Mathematical Methods in the Applied Sciences*, 19(7):555–569, 1996. doi:10.1002/(SICI)1099-1476(19960510)19:7<555::AID-MMA787>3.0.CO;2-X.

[25] Patrizio Frosini and Grzegorz Jabłoński. Combining persistent homology and invariance groups for shape comparison. *Discrete & Computational Geometry*, 55(2):373–409, Mar 2016. doi:10.1007/s00454-016-9761-y.

[26] Patrizio Frosini, Eloy Mósig García, Nicola Quercioli, and Francesca Tombari. Matching distance via the extended Pareto grid. *SIAM J. Appl. Algebra Geom.*, 9(3):554–576, 2025. doi:10.1137/24M1680398.

[27] Patrizio Frosini and Michele Mulazzani. Size homotopy groups for computation of natural size distances. *Bull. Belg. Math. Soc. Simon Stevin*, 6(3):455–464, 1999.

[28] Heather A. Harrington, Nina Otter, Hal Schenck, and Ulrike Tillmann. Stratifying multiparameter persistent homology. *SIAM J. Appl. Algebra Geom.*, 3(3):439–471, 2019. doi:10.1137/18M1224350.

[29] Michael Kerber, Michael Lesnick, and Steve Oudot. Exact computation of the matching distance on 2-parameter persistence modules. *J. Comput. Geom.*, 11(2):4–25, 2020. doi:10.20382/jocg.v11i2a2.

[30] Diogo Lavado, Alessandra Micheletti, Giovanni Bocchi, Patrizio Frosini, and Cláudia Soares. Scenennet: Geometric induction for interpretable and low-resource 3d pole detection with group-equivariant non-expansive operators. *Computer Vision and Image Understanding*, 262:104531, 2025. doi:10.1016/j.cviu.2025.104531.

[31] Michael Lesnick. The theory of the interleaving distance on multidimensional persistence modules. *Found. Comput. Math.*, 15(3):613–650, 2015. doi:10.1007/s10208-015-9255-y.

[32] D. J. Simms. J. Milnor, Morse Theory, Annals of Mathematics Studies 51 (Princeton University Press, 1963), vi + 153 pp., 24s. *Proceedings of the Edinburgh Mathematical Society*, 14(1):84–84, 1964. doi:10.1017/S0013091500011330.

[33] Katharine Turner, Sayan Mukherjee, and Doug M. Boyer. Persistent homology transform for modeling shapes and surfaces. *Information and Inference: A Journal of the IMA*, 3(4):310–344, 2014. doi:10.1093/imaiai/iau011.

[34] Y. H. Wan. Morse theory for two functions. *Topology*, 14(3):217–228, 1975. doi:10.1016/0040-9383(75)90002-6.